ISBN: 978-3-95450-227-1 ISSN: 2673-5490 doi:10.18429/JACoW-IPAC2022-MOPOTK051

MODELING A Nb_3Sn CRYOUNIT IN GPT AT UITF*

S. Pokharel†[1], G. A. Krafft[1]
Center for Accelerator Science, Old Dominion University, Norfolk, Virginia, 23529, USA
A. S. Hofler
Thomas Jefferson National Accelerator Facility, Newport News, Virginia 23606, USA
[1]also at Thomas Jefferson National Accelerator Facility, Newport News, Virginia 23606, USA

Abstract

Nb_3Sn is a prospective material for future superconducting radio frequency (SRF) accelerator cavities. Compared to conventional niobium, the material can achieve higher quality factors, higher temperature operation, and potentially higher accelerating gradients ($E_{acc} \approx 96$ MV/m). In this work, we performed modeling of the Upgraded Injector Test Facility (UITF) at Jefferson Lab utilizing newly constructed Nb_3Sn cavities. We studied the effects of the buncher cavity and varied the gun voltage from 200 –500 keV. We have calibrated and optimized the SRF cavity gradients and phases for the Nb_3Sn five-cell cavities' energy gains with the framework of the General Particle Tracer (GPT). Our calculations show the beam goes cleanly through the unit. There is full energy gain out of the second SRF cavity but not from the first SRF cavity due to non-relativistic phase shifts.

INTRODUCTION

The desire to reduce construction and operating costs of future SRF accelerators motivates the search for higher-performing alternative materials. Nb_3Sn is a very promising alternative material for SRF accelerator cavities. Nb_3Sn possesses a high critical temperature ($T_c \approx 18.3$ K) and superheating field ($H_{sh} \approx 425$ mT) [1,2] giving it the potential for higher intrinsic quality factor (Q_0) than niobium (Nb), 4.2 K operations, and accelerating gradients of ≈ 96 MV/m. Nb_3Sn has a critical temperature about twice that of Nb, allowing it to achieve a high $Q_0 > 10^{10}$ at approximately two times higher operating temperatures than Nb. Changing the operating temperature from 2.0 K, typical for Nb, to 4.3 K for Nb_3Sn while maintaining Q_0 in the 10^{10} to 10^{11} range would reduce energy consumption and thus cryogenic operating costs by as much as an order of magnitude, and would substantially decrease infrastructure costs for the cryogenic plant. Nb_3Sn cavities have a very high quality factor even above 4 K. They can be cooled with cryocoolers for cavity cooling, which significantly cuts capital and installation costs, enabling compact and potentially even mobile applications. Many studies and tests have been done at Thomas Jefferson National Laboratory (JLab) [3–5] for Nb_3Sn and we performed the numerical simulation study of two 5-cell cavities coated with Nb_3Sn through the accelerator layout at UITF for the first time.

* Work supported by U.S. DOE, Office of Science, Office of Nuclear Physics under contract DE-AC05-06OR23177
† spokh003@odu.edu

Based on the UITF beamline layout with a new SRF booster that eliminates the need for a warm capture section, this paper describes the transport of the electron beam through the elements of a 12 m beamline which consist of the photocathode electron gun, solenoids and magnets, buncher cavity, and accelerating superconducting radio frequency (SRF) cavities. With the General Particle Tracer (GPT) [6] simulations, we will describe the designed beam size, the initial electron beam distribution, calibration, and optimization of the Nb_3Sn cryounit using different gun voltages 200 keV, 350 keV, and 500 keV. Also, we will describe the beam properties that would be expected without a capture section.

BEAMLINE SETUP AND SIMULATION DETAILS

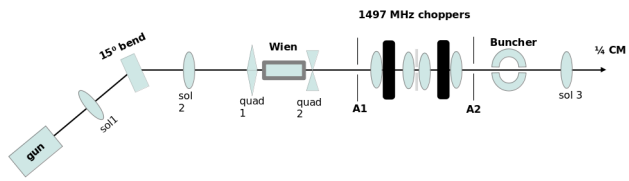

Figure 1: Cathode to the quarter cryomodule (QCM) layout of the Upgraded Injector Test Facility (UITF) at JLab.

Figure 1 is the schematic representation of the keV beamline at the Upgraded Injector Test Facility (UITF) at JLab. The beam dynamics simulation was performed by General Particle Tracer (GPT) [6]. For the simulation, we have used a straight beamline; 15° dipole, RF choppers, beam diagnostics, Wien apertures, etc. are omitted. The laser pulses are getting absorbed by the photocathode inside the electron gun cavity causing the gun to emit the electrons. The electrons are then accelerated to 200 keV initially by the electric field in the DC gun. The electron beam is transported through the solenoids, quadrupoles, and buncher cavity of 750 MHz before reaching the SRF cavities of 1497 MHz. There are two cavities inside the SRF cryomodule, both of them are 5-cell Nb_3Sn cavities separated by 792.79 mm between their centers as shown in Fig. 2. Again, we performed simulations with a different DC gun electric fields to accelerate the beam to 300 keV and 500 keV.

INITIAL DISTRIBUTION

For the particle distribution at the cathode in simulation, the beam is assumed to have a Gaussian distribution in t, x, y, p_x, and p_y following the profile of the laser. The transverse

ISBN: 978-3-95450-227-1 ISSN: 2673-5490 doi:10.18429/JACoW-IPAC2022-MOPOTK051

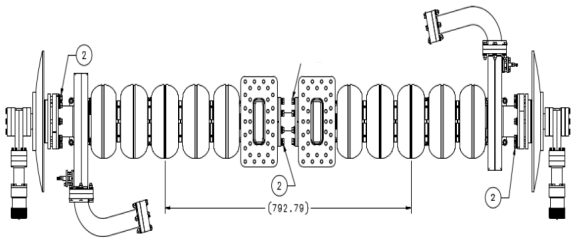

Figure 2: Nb_3Sn pair cryomodule with each of five cells separated by 792.79 mm between their centers [7].

beam size is 213 µm, the laser pulse length is 21.3 ps, and the transverse emittance is 0.061 mmmrad. We have used 1 D profiles for the DC gun and SRF cavities, a 2.5 D field map for RF buncher, and 2 D and 3 D field maps for the solenoids. The beam current used is 1 nA. Thus, the bunch charge is calculated by 1 nA with 750 MHz CW (continuous wave) mode frequency, which is 1.333×10^{-18}C. The applied macro particle number is 2500.

Nb_3Sn UNIT ACCELERATION

We incorporated the buncher cavity into the study and looked at various SRF cavity gradients/phases. The 1 D field map for the cryounit in the simulation is shown in Fig. 3. Using the field map for the cryounit, we first calibrated

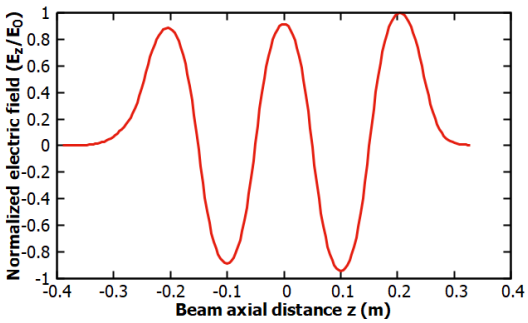

Figure 3: 1 D field map used for Nb_3Sn cryounit in the computer simulation.

the accelerating gradient using the second cavity where the beam is relativistic. Once calibrated, we have optimized the crest phases for each cavity at different accelerating gradients with only the first cavity on. The reason is that the different acceleration rates lead to different phase shifts. Then, the actual energy gains were achieved after cresting had been completed. From the computer simulations, we found that

$$\frac{E_0}{E_{acc}} = 2.1086 \quad (1)$$

for the given field map. Where E_0 is the peak value of the electric field, and E_{acc} is the *accelerating gradient*.

RESULTS AND DISCUSSION

After cresting each of the cavities, the actual energy gains achieved were calculated. The energy gains vs. accelerating gradients are plotted for each of the cavities for different gun voltages 200 kV, 350 kV, and 500 kV. They are shown in Figs. 4 and 5. The energy gain of an arbitrary particle with

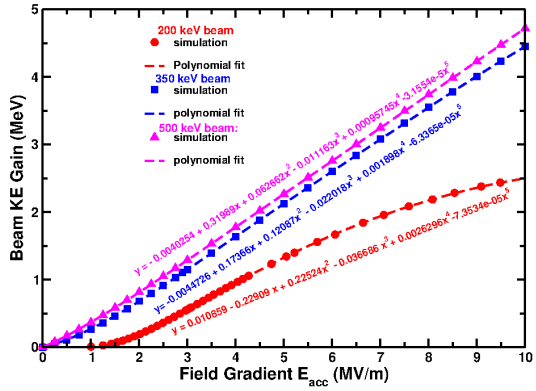

Figure 4: Beam kinetic energy (KE) gain for the first 5-cell cvaity with second five-cell cavity off for different gun voltages 200 kV, 350 kV, and 500 kV.

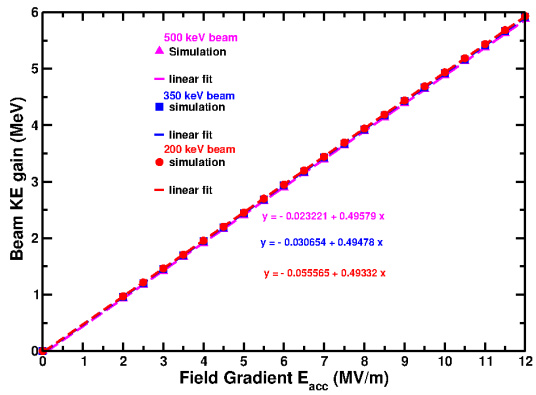

Figure 5: Beam kinetic energy (KE) gain for the second 5-cell cavity (first cavity at 3.6 MV/m) for different gun voltages 200 kV, 350 kV, and 500 kV.

charge e traveling through a SRF gap [8,9] is:

$$\Delta W = e\int_{-\infty}^{\infty} E(0,z)\cos\left(\frac{\omega z}{\beta c} + \phi_s\right) dz = eV_0 T\cos\phi_s \quad (2)$$

where $V_0 = \int_{-\infty}^{\infty} E(0,z)\, dz = E_0 L$ is an axial RF voltage, z is the beam axial distance, L is the effective length of the RF cavity and is given by $L = \beta\lambda_{RF}/2$, and $E_0 T = E_{acc}$, ϕ_s is the synchronous phase of the particle. The transit time factor T is a measure of the reduction of energy gain caused by the sinosoidal time variation of the filed in the SRF gap and is given by

$$T = \frac{\int_{-\infty}^{\infty} E(0,z)\cos\left(\frac{\omega z}{\beta c}\right) dz}{\int_{-\infty}^{\infty} E(0,z)\, dz} - \tan\phi_s \frac{\int_{-\infty}^{\infty} E(0,z)\sin\left(\frac{\omega z}{\beta c}\right) dz}{\int_{-\infty}^{\infty} E(0,z)\, dz} \quad (3)$$

where ω is the RF angular frequency, λ_{RF} is the RF wavelength, β the normalized velocity, and c is the speed of light in vaccum.

ISBN: 978-3-95450-227-1 ISSN: 2673-5490 doi:10.18429/JACoW-IPAC2022-MOPOTK051

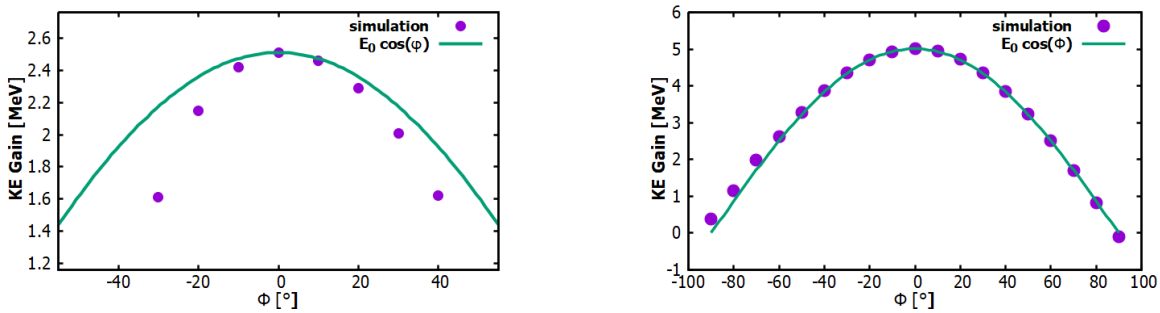

Figure 6: The energy gains vs. phase of-crest (Φ) for the first (left) and second cavity (right) for the accelerating gradient of 10.10 MV/m for 200 keV beam.

For the first 5-cell cavity as shown in Fig.4, the energy gain obtained from the simulation is not linear with the accelerating gradient inside the cavity. The non-linear relation for the beam (200 keV, 350 keV, and 500 keV) is best fitted by the fifth order of the polynomials. However, the best non-linearity is obtained for the 200 keV beam than the 350 keV, and 500 keV cases.

There are several issues to explain the "non-linearity". First, the beam is not relativistic when it enters the cavity as the electrons traversing the cavity are not velocity-of-light and there is phase shifts and incomplete accelerations. The second isssue is the transit time factor. And lastly the effective length of the 5-cell cavity changes for the non-relativistic beam. The cavity length specified $L = \beta\lambda_{RF}/2$ works poorly for low β cavities. So the energy gain is not linear with the field inside the cavity (E_{acc}). For the different settings, the deviation of the energy gain from a linear model in a two-gap RF cavity for a non-relativistic beam was calculated by A. Shemyakin [10]. We observed exactly the same non-linearity for the first 5-cell cavity.

For the second 5-cell cavity, the beam is relativistic and the energy gain obtained from the simulation is linear with the accelerating gradients inside the cavity. The linearity for the beam (200 keV, 350 keV, and 500 keV) are best approximated by the linear fit as shown in Fig. 5.

Again, setting the electric field gradient for both of the 5-cell cavities E_{acc} = 10.10 MV/m, we plotted energy gain vs. the phase off-crest for them for a 200 keV beam which is shown in Figure 6. From the figure, it is clearly seen that there is an incomplete acceleration from the first 5-cell cavity. But the full energy gain is achieved from the second 5-cell cavity as the beam entering the cavity is relativistic. Also, the gain is the cosine function of the phase relative to the crest.

Also, we observed the beam characteristics downstream after the cryounit for the 200 keV beam setting the field gradient (E_{acc}) for the first cavity and second cavity to 3 MV/m and 5 MV/m, respectively. The beam has a bunch length of 1.10 ps, average kinetic energy of 6.86 MeV, and energy spread σ_E of 14.95 keV. The beam envelope (transverse beam sizes and normalized transverse emittances) along the beamline are shown Figs. 7 and 8 respectively.

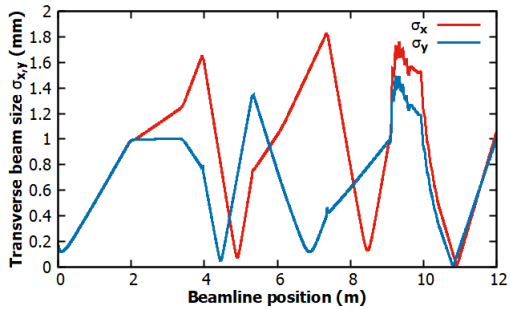

Figure 7: Transverse beam sizes (σ_x and σ_y) for the 200 keV beam.

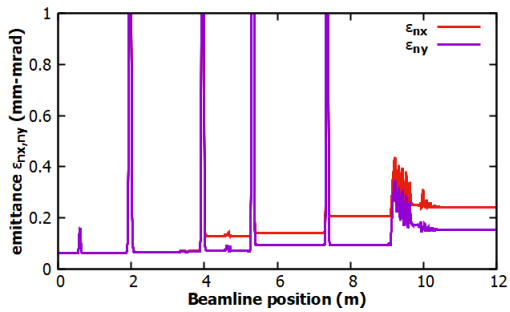

Figure 8: Normalized transverse emittances (ϵ_{nx} and ϵ_{ny}) for the 200 keV beam.

CONCLUSION

We have calibrated and optimized the Nb_3Sn cryounit at UITF at Jefferson Lab using GPT modeling. For all the studied beam cases (200 keV, 350 keV, and 500 keV), the beam goes cleanly through the unit. The beam is not fully relativistic for the first 5-cell cavity; there is no full energy gain out from the cavity. The energy gain is not linear with the field inside the cavity whereas the beam is relativistic for the second 5-cell cavity, there is almost full energy gain out from the cavity. The energy gain is linear with field inside the cavity. Also, we found that using the velocity-of-light structure for the non-relativistic beam is suitable for the desired beam requirement after the quarter cryo-module at Upgraded Injector Test Facility (UITF). Jefferson Lab intends to install such Nb_3Sn cavities in UITF and accomplish the world's first beam acceleration by Nb_3Sn.

ISBN: 978-3-95450-227-1 ISSN: 2673-5490 doi:10.18429/JACoW-IPAC2022-MOPOTK051

REFERENCES

[1] A. Godeke, "A review of the properties of Nb3Sn and their variation with A15 composition, morphology and strain state", *Supercond. Sci. Technol.*, vol. 19, R68–R80, 2006. doi:10.1088/0953-2048/19/8/r02

[2] G. Cetelani and J. P. Sethna, "Temperature dependence of the superheating field for superconductors in the high-κ London limit", *Phys. Rev. B*, vol. 78, p. 224509, 2008. doi:10.1103/PhysRevB.78.224509

[3] U. Pudasaini *et al.*, "Nb3Sn Multicell Cavity Coating at JLab", in *Proc. IPAC'18*, Vancouver, Canada, Apr.-May 2018, pp. 1798–1803. doi:10.18429/JACoW-IPAC2018-WEYGBF3

[4] G. Ciovati *et al.*, "Multi-metallic conduction cooled superconducting radio-frequency cavity with high thermal stability", *Supercond. Sci. Technol.*, vol. 33, 07LT01, 2020. doi:10.1088/1361-6668/ab8d98

[5] G. Eremeev *et al.*, "Nb3Sn multicell cavity coating system at Jefferson Lab.", *Review of Scientific Instruments*, vol. 91, 073911, 2020. doi:10.1063/1.5144490

[6] General Particle Tracer (GPT) code-Pulsar Physics http://www.pulsar.nl/gpt/.

[7] K. Macha, private communication, "JL0041172—C75 same as Nb3Sn pair.pdf", Mar. 2021.

[8] T. P. Wangler, *RF Linear accelerators*, John Wiley & Sons, 2008.

[9] S. Y. Lee, *Accelerator Physics*, Singapore: World Scientific Publishing Company, 2004.

[10] A. Shemyakin, "Energy gain in a two-gap RF cavity", 7 July, 2021. doi:10.48550/arXiv.2107.13041